SAND2019-12631C

Shape-Constrained Input Estimation for Multi-Shaker Vibration Testing

R. Schultz[1,2], P. Avitabile[1]
[1]Department of Mechanical Engineering, University of Massachusetts Lowell, 1 University Avenue, Lowell, MA 01854, USA
[2]Sandia National Laboratories, 1515 Eubank Blvd. SE, Albuquerque, NM 87123, rschult@sandia.gov

Abstract
Multi-shaker vibration testing is effective at accurately replicating complicated field vibration responses in ground tests. Extending this technique to harsher field environments will increase its usage and improve the ability to perform high-fidelity vibration testing with sufficient margin for use in design assessment and even qualification testing. However, achieving higher levels is difficult because of the current state of electrodynamic shakers and multiple-input/multiple-output control algorithms. Here, an improvement is made to the standard multiple-input control algorithm which enables higher response levels to be achieved from a given shaker force level, in some cases in excess of 10 dB. This technique utilizes a set of shape vectors as constraints applied to the various shaker inputs. Pre-defining the relationship, or shapes, of the shaker inputs increases how efficiently the shakers excite the structure.
Simulation studies are utilized to examine this technique, including effects of the number of shape constraints and the use of modes and singular vectors as constraint shapes. Simulation results show shape-constrained input estimation significantly improves the efficiency, or response given some input force, over traditional control techniques.

Keywords: multi-shaker testing, MIMO, vibration testing, control algorithm, input estimation

1. Introduction

Multi-shaker vibration testing has shown promise in accurately replicating the vibration response for components or systems subject to complicated field environments [1, 2, 3]. Using multiple shakers along with a multiple-input/multiple-output (MIMO) controller allows for the response of the device under test (DUT) to be matched at more locations than traditional single-axis vibration tests because there is more controllability. One challenge with multi-shaker testing is how to efficiently coordinate the shakers to provide high-level response from shakers with limited capabilities. The typical MIMO direct control approach simply attempts to match the target response, without any provisions on the inputs required to do so. Here, a modification is presented to the direct control, or input estimation, equation which coordinates the various shakers through a set of specified constraint shapes. This technique, dubbed shape-constrained input estimation, can utilize any set of vectors for constraints though here the focus is on mode shapes and right singular vectors of the frequency response function (FRF) matrix.

2. MIMO Input Estimation

Consider the linear system:

$$\{Y\} = [H]\{X\}, \tag{1}$$

which is represented by vectors of the linear spectra of the N inputs, $\{X\}$, M outputs, $\{Y\}$, and an MxN system FRF matrix, $[H]$. For stationary random vibration problems, this is typically written in power space:

$$[S_{yy}] = [H][S_{xx}][H]^H, \tag{2}$$

where the inputs and outputs are written in terms of the cross-power spectral density (CPSD) matrices $[S_{xx}]$ and $[S_{yy}]$, respectively, and $[\square]^H$ denotes the conjugate transpose, or Hermitian, of the matrix [4].

Sandia National Laboratories is a multimission laboratory managed and operated by National Technology & Engineering Solutions of Sandia, LLC, a wholly owned subsidiary of Honeywell International Inc., for the U.S. Department of Energy's National Nuclear Security Administration under contract DE-NA0003525.

Typical direct input estimation of this MIMO linear system is performed as [5]

$$[S_{xx1}] = [H]^{+}[S_{yy0}][H]^{+H}. \tag{3}$$

This requires a pseudo-inverse of the FRF matrix, denoted by $[\square]^{+}$, which means the estimated inputs, $[S_{xx1}]$, are the inputs which would produce outputs, $[S_{yy1}]$, which best match the target outputs, $[S_{yy0}]$, in a least-squares sense. The resulting outputs, $[S_{yy1}]$, come from the application of the estimated inputs to Equation 2. Clearly, there is no attempt to tailor the inputs in a specific way; the inputs are simply those which best match the response in a least-squares sense. Indeed, often times the estimated inputs are in excess of shaker force capabilities.

3. Application of Constraints on Inputs

In an effort to reduce shaker force requirements, shape-constrained input estimation was developed. This input estimation technique modifies the typical MIMO input estimation equation by applying a constraint matrix, $[C]$, to the FRF matrix as

$$[\hat{H}] = [H][C], \tag{4}$$

resulting in a constrained FRF matrix, $[\hat{H}]$. This constrained FRF matrix is then used to estimate a set of constrained inputs whose dimensions are smaller than the full set of unconstrained inputs. That is, for N unconstrained inputs, there will be fewer constrained inputs, $\hat{N} < N$. The shape-constrained input estimation equation is then

$$[\hat{S}_{xx1}] = [\hat{H}]^{+}[S_{yy0}][\hat{H}]^{+H}. \tag{5}$$

Converting from constrained inputs to full inputs is done by applying the constraint matrix to the estimated, constrained inputs:

$$[S_{xx1}] = [C][\hat{S}_{xx1}][C]^{H}. \tag{6}$$

The content in the constraint matrix is simply one or more shape vectors. With a single vector, the constraint is strict and directly relates all the inputs together, enforcing the inputs (forces or voltages) to fit that shape. With more vectors, there is a blending of the shapes. While these shape vectors can be anything, there are advantages to using specific types of vectors, as will be shown in the following sections.

3.1. Mode Shape Constraints

Say a system has mode shapes $\{U_1\},\{U_2\},...,\{U_k\}$ that form the mode shape matrix $[U]$. A subset of those modes can be used as shape constraints by populating the constraint matrix with one or more mode shape vectors. For example a constraint matrix using mode 1 and mode 2 would be

$$[C] = [\{U_1\}\{U_2\}]. \tag{7}$$

In this case, the inputs will be constrained to resemble a combination of the two mode shapes. In this way, the inputs can be forced to mimic the natural deflection patterns of the structure, which can have advantages where the response is dominated by a single mode or a small number of modes.

3.2. Singular Vector Constraints

Mode shapes for constraint vectors presents a couple of practical problems. First, the mode shapes must be known, meaning a modal test needs to be run and modes extracted. Second, the mode or modes to be used as constraint vectors must be chosen at each frequency line. Alternatively, the singular vectors of the DUT FRF matrix can be used in place of mode shapes. The singular value decomposition of the FRF matrix is:

$$[H] = [U_\Sigma][S_\Sigma][V_\Sigma]^{H}, \tag{8}$$

where $[U_\Sigma],[V_\Sigma]$ are the left and right singular vector matrices, respectively, and $[S_\Sigma]$ is a diagonal matrix of singular values. The left singular vectors are the “shapes” at the output degrees of freedom (DOFs) and the right singular vectors are the “shapes” at the input DOFs. So, one or more right singular vectors can be used to constrain the shakers (inputs) with one or more constraint shapes. As the singular values and vectors are a function of frequency, the singular value decomposition can be performed at each frequency line, providing new singular vectors and thus new constraint vectors at each frequency line automatically. In this way, the constraint matrix can be a function of frequency, with the vectors in the matrix changing each frequency line. For example, for two right singular vector constraints, the constraint matrix would be:

$$[C]=\left[\{V_{\Sigma,1}\}\{V_{\Sigma,2}\}\right]. \quad (9)$$

Because singular vectors are orthonormal, the use of singular vectors as constraints applied to the FRF matrix results in truncation of the non-constraint singular values and vectors. That is, the constrained FRF matrix, $[H][C]$, can be written in terms of the product of the constrained singular values and vectors. For example, if the top two singular vectors are used as constraints, the constrained FRF matrix can be written as:

$$[H][C]=\left[\{U_{\Sigma,1}\}\{U_{\Sigma,2}\}\right]\begin{bmatrix} S_{\Sigma,1} & 0 \\ 0 & S_{\Sigma,2} \end{bmatrix}\left[\{V_{\Sigma,1}\}\{V_{\Sigma,2}\}\right]^{H}. \quad (10)$$

This indicates that shape-constrained input estimation using singular vectors is essentially a rank reduction regularization method [6, 7]. It should be noted that typical regularization approaches aim to only change the very smallest singular values to avoid numerical error propagation issues, however in this context the regularization is very strong, keeping only the very largest singular values to enforce a particular pattern or shape constraint on the inputs.

4. Demonstration of Shape-Constrained Input Estimation

Shape-constrained input estimation will be compared with standard input estimation using a contrived, although representative dynamic system. This system is first subjected to a complicated set of field loads, generating a target response at some DOF. Next, forces (shakers) will be used to try and replicate that target field response with each shaker input determined with either standard or shape-constrained input estimation. The effects of using modes or singular vectors, as well as the effects of the number of constraint vectors, will be examined with this example system.

4.1. Example System

A cantilever beam is chosen as the example system here because it has dynamics that are familiar and intuitive. This beam is 2.54 cm square and 101 cm long with aluminum material properties and an assumed two percent modal damping on all modes. Twenty elements are used to model the transverse bending of the beam, Figure 1. Five output DOFs were chosen, at nodes 4, 6, 9, 10, and 19. To simulate a field environment and generate the target response at those five output DOFs, uniform random (uncorrelated) forces were applied to each node between 0 and 800 Hz. This bandwidth covers the first four modes and allows the main features of the response to be examined. To simulate the laboratory, multi-shaker, test configuration, four shaker forces were applied at nodes 3, 8, 12, and 14. While the locations of inputs and outputs do affect results of this type of problem, for simplicity these locations were chosen arbitrarily.

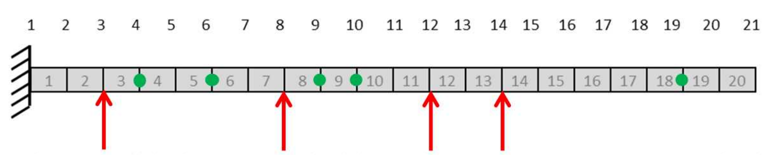

Figure 1: Diagram of the beam model with 20 elements, 5 output DOFs, and 4 input DOFs

4.2. Modes vs. Singular Vectors for Constraint Shapes

Mode shapes as constraint shapes makes sense intuitively, however using singular vectors has the advantage of being automatically frequency-variable and coming directly from the FRF matrix which is already being measured in a test. Thus, a comparison of the performance of mode shapes and singular vectors as constraints is useful. First, the modes and right singular vectors of this beam were examined. Figure 2 shows the first four modes of the beam and the top right singular vectors at the mode frequency. Because the singular vectors are complex, the plot shows the signed magnitude. Indeed, the right singular vector shapes closely resemble the mode shapes, indicating they may be useful as constraint shapes.

Figure 3 shows results of a multi-shaker input estimation simulation using shape-constrained input estimation to determine the inputs to the four shakers to best match the random force target environment. A single mode shape or singular vector was used as the constraint matrix in this example. The mode constraint shape at each frequency line was chosen as the mode with frequency nearest that frequency line. As there are five outputs and four inputs over a broad frequency range, there is too much data to plot in full. Instead, Figure 3 shows the trace, or sum of the five output power spectral densities (PSDs) (a), the mean dB error in the PSDs of all the outputs (b), individual gauge PSDs (c,d), and the root mean square (RMS) response (e) and input (f).

Examining the response PSDs in (a-d) indicates that the response is well matched near the peaks of the four modes, with some error between the peaks. The response between peaks is typically due to a combination of two or more modes, so constraining the inputs to just a single shape reduces the accuracy in these regions. The RMS response in (e) shows that overall the response is very closely matched with the target response at all five outputs and the RMS input force in (f) indicates that the required forces using either mode shapes or singular vectors as constraints is roughly equal.

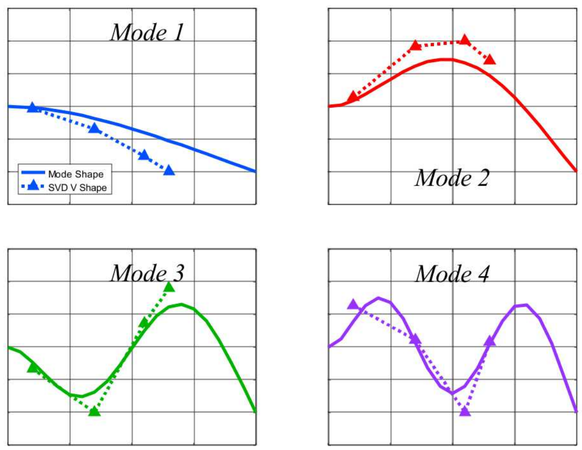

Figure 2: First four mode shapes (solid) and the right singular vectors (dotted) at the mode frequencies

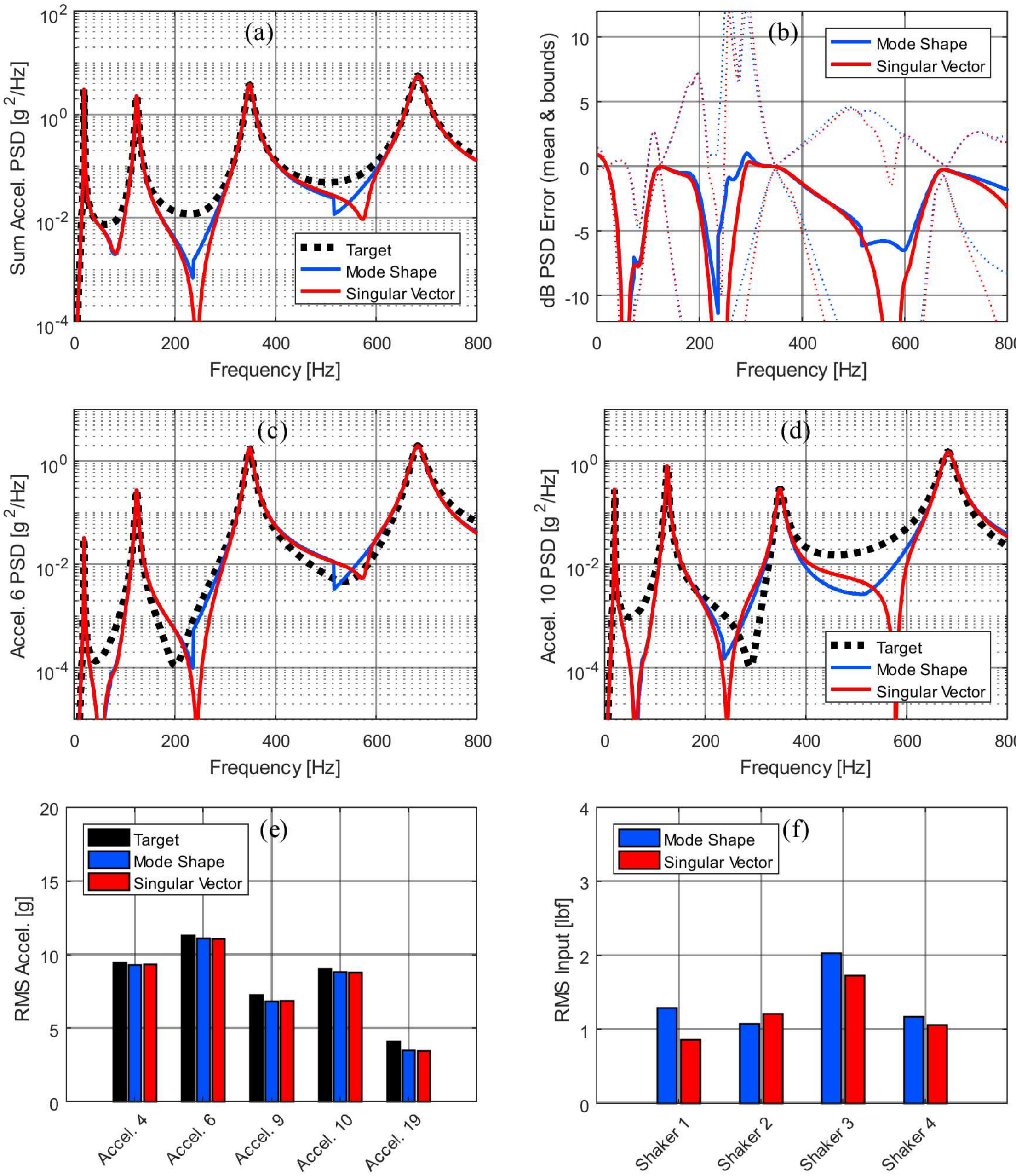

Figure 3: Response and input results for the multi-shaker simulation comparing a single mode or singular vector constraint. (a) Sum of five output PSDs. (b) Mean dB error of the five output PSDs. (c) Output PSD at node 6. (d) Output PSD at node 10. (e) RMS output at five nodes. (f) RMS force at four inputs.

4.3. Effects of the Number of Constraint Vectors

While the number of constraint vectors in the constraint matrix can be anything from one to the number of inputs, the number affects the response and inputs. To demonstrate this, the constraint matrix was formed with one, two, or three right singular vectors. As in Figure 3, Figure 4 shows the results of this simulation in terms of different response (a-e) and input (f) metrics. There is a clear trend, with response accuracy improving with an increasing number of constraint vectors. Using two or three vectors, in this case, results in a very close match to the target response, even between peaks. Going from two to three vectors yields a slightly more accurate result in terms of the PSDs, however the RMS values are basically unchanged. There is a marked difference in the required inputs, however, with the three-vector case requiring much higher input force than the two-vector case. The two-vector case does require more input force than the one vector case but does come with a significant improvement in response accuracy across the bandwidth. Thus, there is a balance between response accuracy and input force which is controlled by the number of constraint vectors used in shape-constrained input estimation.

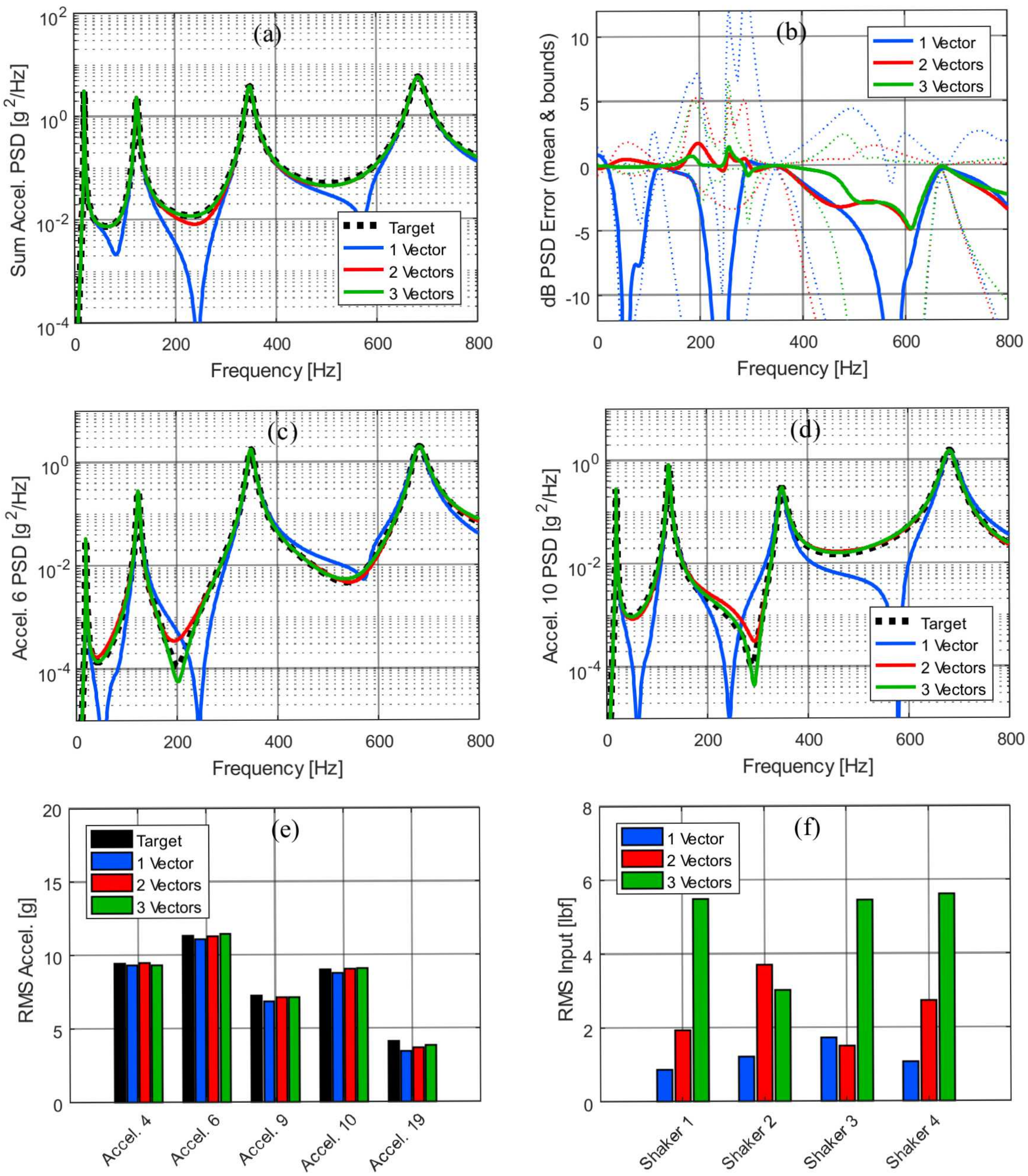

Figure 4: Response and input results for the multi-shaker simulation comparing one, two, and three singular vector constraints. (a) Sum of five output PSDs. (b) Mean dB error of the five output PSDs. (c) Output PSD at node 6. (d) Output PSD at node 10. (e) RMS output at five nodes. (f) RMS force at four inputs.

4.4. Comparison with Standard Input Estimation

With some understanding of how shape-constrained input estimation works and its sensitivity to the type and number of constraint vectors, a comparison can be made with standard input estimation (Equation 3). Here, shape-constrained input estimation is implemented using two right singular vectors for all frequency lines. Figure 5 shows the same response and input plots as shown for the cases above. The responses (a-e) indicate that standard input estimation yields a response which very nearly matches the target response overall and on a gauge-by-gauge basis. The response from shape-constrained input estimation also matches the target response well, and particularly around the peaks. The RMS values are very close to the target levels for each gauge. The RMS input force (f) shows a dramatic difference in the required force, particularly for shaker 3 and 4 where shape-constrained input estimation is several times lower than standard input estimation. In this particular case, the difference is upwards of 18dB for shaker 3. Similar input level reductions have been observed with shape-constrained input estimation applied to various contrived and actual dynamic systems and environments.

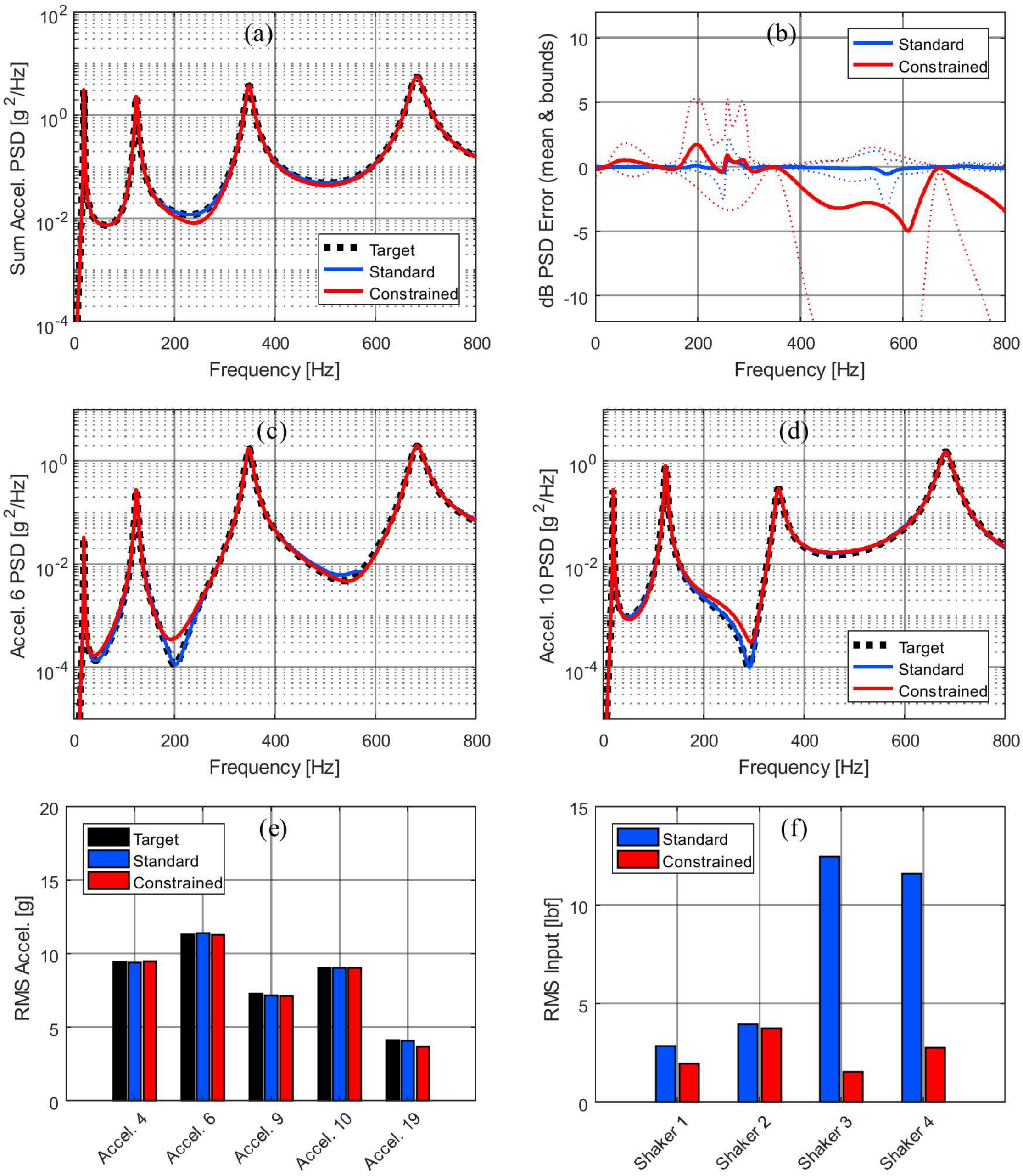

Figure 5: Response and input results for the multi-shaker simulation comparing standard and shape-constrained input estimation. (a) Sum of five output PSDs. (b) Mean dB error of the five output PSDs. (c) Output PSD at node 6. (d) Output PSD at node 10. (e) RMS output at five nodes. (f) RMS force at four inputs.

5. Conclusions

A need to improve the efficiency and response levels in multi-shaker vibration testing motivated the development of a new input estimation method. Shape-constrained input estimation utilizes a modification of the standard MIMO input estimation equation, where the FRF matrix is multiplied by a constraint matrix. This constraint matrix enforces a pattern on the inputs, resulting in higher response levels. While the constraint shapes can be any vector in theory, here mode shapes and right singular vectors of the FRF matrix were explored. It was found that right singular vectors perform as well as mode shapes and have the benefits of not needing a modal test and automatically changing with each frequency line. Also, it was found that the number of constraint vectors controls a balance between response accuracy and input force, with more accuracy and higher force coming with more constraint vectors. However, even with a single constraint shape the response is very accurate around the peaks in the response and thus captures the majority of the response energy accurately. Finally, shape-constrained input estimation was found to be nearly as accurate as standard input estimation while greatly reducing the required forces, with the reduction for some shakers greater than 10 dB.

References

[1] P. M. Daborn, "Scaling up of the Impedance-Matched Multi-Axis Test (IMMAT) Technique," in *Proceedings of IMAC XXXV, the 35th International Modal Analysis Conference*, Garden Grove, CA, 2017.

[2] R. L. Mayes and D. P. Rohe, "Physical Vibration Simulation of an Acoustic Environment with Six Shakers on an Industrial Structure," in *Proceedings of IMACXXIV, the 34th International Modal Analysis Conference*, 2016.

[3] C. Roberts and D. J. Ewins, "Multi-axis vibration testing of an aerodynamically excited structure," *Journal of Vibration and Control,* vol. 24, no. 2, pp. 427-437, 2018.

[4] J. S. Bendat and A. G. Piersol, Random Data: Analysis and Measurement Procedures, John Wiley & Sons, 2010.

[5] J. O'Callahan and F. Piergentili, "Force Estimation Using Operational Data," in *Proceedings of IMAC XIV, the 14th International Modal Analysis Conference*, 1996.

[6] A. E. Yagle, "Application Note: Regularized Matrix Computations, Department of EECS, the University of Michigan," [Online]. Available: http://web.eecs.umich.edu/~aey/recent/regular.pdf. [Accessed 2017].

[7] O. Krause and C. Igel, "A more efficient rank-one covariance matrix update for evolution strategies," in *Proceedings of FOGA2015, Foundations of Genetic Algorithms XIII*, Wales, UK, 2015.

[2]Sandia National Laboratories is a multimission laboratory managed and operated by National Technology & Engineering Solutions of Sandia, LLC, a wholly owned subsidiary of Honeywell International Inc., for the U.S. Department of Energy's National Nuclear Security Administration under contract DE-NA0003525.